

# In vitro anti-hepatocellular carcinogenesis of 1,2,3,4,6-Penta-O-galloyl- $\beta$ -D-glucose

**Yuhan Jiang**

Wuhan Polytechnic University

**Jing-hui Bi**

Wuhan Polytechnic University

**Min-rui Wu**

Wuhan Polytechnic University

**Shi-jie Ye**

Wuhan Polytechnic University

**Yang Yi**

Wuhan Polytechnic University

**Hong-xun Wang**

Wuhan Polytechnic University

**Li-mei Wang** (✉ [wanglimeiyx@163.com](mailto:wanglimeiyx@163.com))

Wuhan Polytechnic University

---

## Research Article

**Keywords:**  $\beta$ -PGG, apoptosis, hepatocellular carcinoma, network pharmacology, p53 signaling pathway

**Posted Date:** May 18th, 2022

**DOI:** <https://doi.org/10.21203/rs.3.rs-1645156/v1>

**License:**  This work is licensed under a Creative Commons Attribution 4.0 International License.

[Read Full License](#)

---

# Abstract

The main aim of this study was to explore the antitumor effects and mechanism of 1,2,3,4,6-Penta-O-galloyl- $\beta$ -D-glucose on human hepatocellular carcinoma HepG2 cells. A network pharmacology method was first used to predict the possible inhibition of hepatocellular carcinoma growth by  $\beta$ -PGG through the p53 signaling pathway. Next, the CCK-8 assay was performed to evaluate changes in the survival rate of human hepatocellular carcinoma HepG2 cells treated with different concentrations of the drug; flow cytometry was used to detect changes in cell cycle, apoptosis, mitochondrial membrane potential, and intracellular  $\text{Ca}^{2+}$  concentration; and real-time fluorescence quantification and immunoblotting were performed to evaluate changes in the expression of *P53*, *BAX*, and *BCL-2*. Results showed that the expression of *P53* genes and proteins associated with the p53 signaling pathway was significantly increased by  $\beta$ -PGG treatment. It was found that  $\beta$ -PGG significantly inhibited survival of HepG2 cells, promoted apoptosis, decreased mitochondrial membrane potential and intracellular  $\text{Ca}^{2+}$  concentration, upregulated *P53* gene and protein expression, increased *CASP3* expression, and induced apoptosis in HepG2 cells. In conclusion, this study has shown that network pharmacology can accurately predict the target of  $\beta$ -PGG's anti-hepatocellular carcinoma action. Moreover, it was evident that  $\beta$ -PGG can induce apoptosis in HepG2 cells by activating the p53 signaling pathway to achieve its anti-hepatocellular carcinoma effect *in vitro*.

## 1. Introduction

Cancer is considered to be the greatest challenge to human life and health. Liver cancer, as the third most deadly malignancy in the world, causes about 383,000 deaths each year in China, and its late detection and poor prognosis pose a serious threat to public life and health<sup>1-3</sup>. Studies have revealed that viral infections, metabolic diseases, and diet are important risk factors for development of liver cancer, with dietary factors leading the list<sup>4</sup>. Consequently, prevention of cancer by food and nutrients has become a research hotspot. Over the years, a number of macronutrients, micronutrients, and non-nutrients have been reported to play an important role in cancer prevention<sup>5</sup>, and natural ingredients derived from food have been shown to be more advantageous than synthetic compounds in the fight against tumours<sup>6</sup>. Therefore, it is of great significance to elucidate the underlying molecular mechanism of natural ingredients against liver cancer, with the overarching goal of identifying molecular targets for the targeted therapy of liver cancer.

Polyphenols are common micronutrients in the diet and have significant therapeutic effects on degenerative diseases, such as cancer and certain cardiovascular diseases<sup>7</sup>. 1,2,3,4,6-Penta-O-galloyl- $\beta$ -D-glucose ( $\beta$ -PGG) is a polyphenol ellagic compound present in numerous foods, including pomegranate, rhizome, mango, and other foods with polyphenolic properties<sup>8</sup>. It has shown strong biological and pharmacological activities in antiviral<sup>9</sup>, anti-inflammatory<sup>10</sup>, anti-microbial<sup>11</sup>, and anti-diabetic<sup>12</sup>. Previous studies have shown that  $\beta$ -PGG exhibits inhibitory effects on colon cancer<sup>13</sup>, breast cancer<sup>14</sup>,

prostate cancer<sup>15</sup>, and pancreatic cancer<sup>16</sup>. However, there is a lack of reports on the anti-hepatocellular carcinoma effects of  $\beta$ -PGG and the possible mechanisms.

Network pharmacology is a drug design approach that encompasses systems biology, network analysis, connectivity, redundancy, and pleiotropy, and thus it can support the development of new drugs as well as explore biological mechanisms. Specifically, network pharmacology reveals the network of drug-gene-disease interactions, and further reflects the multi-target and multi-pathway nature of drug therapy<sup>17</sup>.

In view of this, this study used network pharmacology to screen the possible targets of  $\beta$ -PGG against hepatocellular carcinoma and to systematically predict its molecular mechanism of action. We expect that this study will provide a basis for the development and application of functional foods for treating liver cancer.

## **2. Materials And Methods**

### **2.1 Network pharmacology experimental predictions**

#### **2.1.1 $\beta$ -PGG and liver cancer target prediction and screening application**

The 2D structure of  $\beta$ -PGG was obtained from Pubchem database, and then the sdf file of the drug structure was imported into PharmMapper and SwissTargetPrediction databases to merge and de-duplicate the drug-related targets. Next, disease related targets were obtained from the GeneCards database using the keyword "liver cancer", with "human" as the genus.

#### **2.1.2 Acquisition of crossover genes and construction of protein-protein interaction (PPI) networks**

The intersection of  $\beta$ -PGG targets with liver cancer targets was determined using JVENN software. The intersecting targets were then entered into the Protein Interaction Database (STRING) setting the species origin to human and the minimum relationship score to 0.4. Notably, the free proteins were removed to obtain the protein interactions map.

#### **2.1.3 Acquisition of HUB genes and GO and KEGG enrichment analyses**

The protein interactions maps obtained from the STRING database were imported into Cytoscape 3.7.1 software and then the MCC calculation method in the CytoHubba plugin<sup>18</sup> was utilized to obtain the top eight central target proteins in the network. The central target proteins were then subjected to gene ontology (GO) and Kyoto Encyclopedia of Genes and Genomes (KEGG) analyses using the R package clusterProfiler<sup>19</sup>. Enrichplot<sup>20</sup> R package was used to filter out data with  $p$ -value < 0.05, and finally ggplot2<sup>21</sup> R package was applied to plot the relevant legends.

## **2.2 *In vitro* experiments**

### **2.2.1 Materials and reagents**

Hepatocellular carcinoma cell line HepG2 were purchased from Biyuntian Biotechnology Co. Ltd.; DNA content assay kit, mitochondrial membrane potential assay kit (JC-10), and calcium ion assay kit were supplied by Beijing Solabao Technology Co. Ltd.; T25 cell culture flasks, 96-well plates, lyophilization tubes, and six-well plates were obtained from Corning, USA; and western blot-related antibodies were purchased from Wuhan Seville Biotechnology Co.

### **2.2.2 Instruments and equipment**

SIM CO<sub>2</sub> incubator, SIM, USA; Inverted microscope, Olympus, Japan; Infinite200PRO enzyme marker, TECAN, Switzerland; Flow cytometer, Beckman coulter, USA; Thermal cycling PCR, real-time fluorescence quantitative PCR, gel imager and electrophoresis instrument, Bio-Rad, USA.

### **2.2.3 Cell culture**

Human hepatocellular carcinoma HepG2 cells were cultured in DMEM medium supplemented with 10% fetal bovine serum to provide nutrients and 1% double antibiotics to prevent contamination of the medium. Cells were grown to about 80% confluence in a 1:3 ratio of passaged culture.

### **2.2.4 Cell proliferation assay**

Cell proliferation was detected by the Cell Counting Kit (CCK-8). Briefly, HepG2 cells were inoculated at a density of  $4 \times 10^4$  cells/well using complete medium in 96-well plates and incubated overnight. On the next day, the medium was aspirated and equal amounts of  $\beta$ -PGG (0, 12.5, 25, 50, 100, and 200  $\mu$ g/mL) and 5-FU (positive control) were added, followed by incubation for 24 h or 48 h. Next, the medium was removed, 10  $\mu$ l of CCK-8 was added to each well, and incubated at 37°C for 4 h. The optical density (OD) of each well was then measured at 450 nm by enzyme marker.

### **2.2.5 Cell cycle assay**

PI staining was used to detect cell cycle distribution. Briefly, HepG2 cells were digested and inoculated overnight in 6-well plates until they reached 80% of the culture flask, and then they were cultured with a gradient concentration of  $\beta$ -PGG for 48 h. Next, trypsin digestion was performed, cell concentration was adjusted to  $1 \times 10^6$  cells/mL with PBS, and cells were fixed in 70% ethanol at -20°C overnight. On the next day, cells were collected and washed in cold PBS, and resuspended in 0.5 mL PBS. Cells were then treated with Rnase A solution for 30 min to fully degrade the RNA, followed by PI staining to determine the cell cycle phase using flow cytometry.

### **2.2.6 Apoptosis detection**

Apoptosis was detected by the Annexin V-FITC/PI double staining method. In brief, the cell concentration was adjusted to  $2 \times 10^6$  cells/mL, 2 mL of the cells were inoculated in a 6-well plate, and then they were washed with PBS after 24 h and incubated with equal amounts of different concentrations of  $\beta$ -PGG for 48 h. After digestion with EDTA-free trypsin, cells were collected and resuspended by adding 400  $\mu$ L AnnexinV conjugate followed by 5  $\mu$ L of FITC. PI staining was then performed at 4 °C, with protection from light, and finally cell apoptosis was detected by flow cytometry.

## 2.2.7 Determination of mitochondrial membrane potential

The intracellular mitochondrial membrane potential was detected by JC-10 staining method. The cell concentration was first adjusted to  $2 \times 10^6$  cells/mL, 2 mL of the cells were then inoculated in 6-well plates, followed by treating with different concentrations of  $\beta$ -PGG for 48 h. Next, the complete medium was adjusted to  $1 \times 10^6$  cells/mL and 1 mL of JC-10 staining working solution was added to stain the cells at 37°C. Finally, the stained cells were resuspended using 1 $\times$  of JC-10 staining buffer and then detected by flow cytometry.

## 2.2.8 Intracellular calcium ion concentration assay

Cell suspensions from the passaged cultures were adjusted to a cell concentration of  $2 \times 10^6$  cells/mL and 2 mL of the cells was incubated in 6-well plates for 24 h. Cells were then treated with different concentrations of  $\beta$ -PGG. After incubation for 48 h, cells were collected for subsequent probe loading operations. Finally, cells were washed and resuspended using HBSS pre-warmed to 37°C, and then detected by flow cytometry.

## 2.2.9 Gene expression detection by qRT-PCR

This study performed real-time fluorescence quantification of relevant genes on the pathway predicted by network pharmacology. Briefly, HepG2 cells were inoculated in culture flasks and treated for 48 h with  $\beta$ -PGG dissolved in complete medium to a concentration of 100  $\mu$ g/mL. RNAiso Plus kit was then used to extract total RNA from HepG2 cells in accordance with the manufacturer's instructions. Next, the extracted RNA was reverse transcribed on ice into cDNA using the Prime-script RT Master Mix kit according to the manufacturer's protocol. qRT-PCR analysis was then performed using the SYBR Green Master Mix kit with the  *$\beta$ -actin* gene as an internal reference. (Table 1 shows sequences of the used PCR amplification primers)

Table 1  
PCR primer sequence

Gene	Forward primer (5'→3')	Reverse primer (5'→3')
PUMA	GAGGAGGAACAGTGGGCC	GGAGTCCCATGATGAGATTGT
Bax	AAGAAGCTGAGCGAGTGTCT	GTTCTGATCAGTTCCGGCAC
Bcl-2	GCCTTCTTTGAGTTCGGTGG	GAAATCAAACAGAGGCCGCA
Caspase-3	ACTGGACTGTGGCATTGAGA	GCACAAAGCGACTGGATGAA
Caspase-9	GCCCCATATGATCGAGGACA	CAGAAACGAAGCCAGCATGT
P21	GACACCACTGGAGGGTGACT	CAGGTCCACATGGTCTTCCT
P53	GTTCCGAGAGCTGAATGAGG	TCTGAGTCAGGCCCTTCTGT
IGF-BP3	CCTGCCGTAGAGAAATGGAA	AGGCTGCCCATACTTATCCA
PERP	TGCCATCATTCTCATTGCAT	AACCCAGTTGAACTCATGG
Cytochrome c	ATGAAGTGTTCCAGTGCCA	CTCTCCCAGATGATGCCTT
β-Actin	CATCCGCAAAGACCTGTACG	CCTGCTTGCTGATCCACATC

## 2.2.10 Protein immunoblotting to determine protein expression

HepG2 cells were treated with 100 µg/mL β-PGG for 48 h. At the end of the treatment, cells were washed twice with TBS buffer and fully lysed with Total Protein Extraction Reagent. The cell debris was collected and the cell supernatant was collected by centrifugation at 12000 r/min for 15 min to obtain the total protein solution. The protein concentration was determined using the BCA kit and then samples were resolved using electrophoresis. Samples were spotted on a pre-prepared gel plate, closed by transferring the membrane, incubated with antibody, and developed in a developer using the chemiluminescence ECL kit.

## 2.2.11 Statistical analyses

All statistical analyses were performed using GraphPad Prism 8.0.2 software and all data are expressed as the mean ± SD of three independent experiments. For all experiments, *p*-value < 0.05 was considered statistically significant.

## 3. Results

## 3.1 Acquisition and network construction of $\beta$ -PGG targets for the treatment of hepatocellular carcinoma

The 3D structure of  $\beta$ -PGG was retrieved from the PubChem database (Fig. 1a). A total of 372 genes associated with  $\beta$ -PGG were obtained from PharmMapper and SwissTargetPrediction databases, whereas 16731 liver cancer-related genes were obtained from the GeneCards database. A total of 363 crossover genes were obtained after intersection of drug genes and disease genes (Fig. 1b), suggesting that  $\beta$ -PGG may regulate the progression of hepatocellular carcinoma through these crossover genes. To further evaluate the interrelationship between  $\beta$ -PGG and hepatocellular carcinoma, a " $\beta$ -PGG-target-hepatocellular carcinoma" network was constructed in Cytoscape 3.7.1 software (Fig. 1c).

## 3.2 Construction of PPI networks and acquisition of HUB genes

Cytoscape software was used to visualize the protein interactions, whereas the MCC calculation method in the CytoHubba plugin was applied to calculate the top eight target genes of the protein interactions network, namely *TP53*, *IGF1*, *EGFR*, *VEGFA*, *CASP3*, *MMP2*, *MMP9*, and *SRC* (Fig. 2). Results suggested that the above genes and related proteins play a crucial role in the liver cancer treatment.

## 3.3 GO and KEGG enrichment analyses

To elucidate the mechanism of  $\beta$ -PGG action on hepatocellular carcinoma, the eight HUB genes were subjected to enrichment analysis using R studio. Figure 3 shows the GO enrichment results which indicate that the hub genes were mainly associated with biological processes, such as negative regulation of apoptotic process, positive regulation of DNA binding, and positive regulation of mitochondrial Cytochrome c release. On the other hand, the KEGG results revealed that the genes were mainly associated with signaling pathways such as RAP1 and p53. The combined GO and KEGG analyses demonstrated that  $\beta$ -PGG inhibits hepatocellular carcinoma by inducing apoptosis, where *P53*, as an important oncogene, regulates the cell cycle and prevents cell carcinogenesis<sup>22</sup>; whereas *CASP3*, as an executor of apoptosis, can remove damaged cells and catalyze cleavage of many key cellular proteins to achieve apoptosis after being activated<sup>23</sup>. In summary, the p53 signaling pathway, which is most closely associated with apoptosis, was selected for further validation.

## 3.4 Effect of different concentrations of drugs on the inhibition rate of hepatocellular carcinoma HepG2 cells

Figure 4 shows that the proliferation inhibition rate of  $\beta$ -PGG on HepG2 cells was concentration-dependent, and the inhibition rate was positively correlated with the drug concentration. The obtained results demonstrated that the effect of  $\beta$ -PGG was better than that of 5-FU under the experimental conditions of drug treatment for 24 h and concentrations of 50–200  $\mu$ g/mL. However, there was no

significant difference between the effect of  $\beta$ -PGG and 5-FU under the experimental conditions of drug treatment for 48 h and concentrations of 100–200  $\mu\text{g}/\text{mL}$ . The drug effects were further evaluated by calculating the  $\text{IC}_{50}$  values of each group. Results showed that the  $\text{IC}_{50}$  of  $\beta$ -PGG treated HepG2 cells for 24 h and 48 h were 40.85 and 28.50, respectively, whereas the  $\text{IC}_{50}$  of 5-FU treated HepG2 cells for 24 h and 48 h were 42.95 and 21.06, respectively. Based on the  $\text{IC}_{50}$  results, it was evident that  $\beta$ -PGG and 5-FU were equally effective. In addition, it was found that the longer the treatment time, the stronger the killing effect on HepG2. Collectively, these results suggest that  $\beta$ -PGG inhibited proliferation of human hepatocellular carcinoma HepG2 cells and showed a good dose-effect relationship.

### **3.5 Effect of $\beta$ -PGG on the HepG2 cell cycle in hepatocellular carcinoma**

Figure 5 shows that the number of hepatocellular carcinoma cells in G2/M phase decreased in a dose-dependent manner after 48 h of intervention with different concentrations of  $\beta$ -PGG. The proportion of S phase increased when the concentration of the drug was less than 50  $\mu\text{g}/\text{mL}$ , whereas the proportion of G0/G1 phase increased when the concentration was greater than 50  $\mu\text{g}/\text{mL}$ . These results suggested that the low concentration of  $\beta$ -PGG blocked growth of HepG2 cells in S-phase, whereas the increased concentration of the drug blocked growth of the cells in G0/G1-phase, thereby achieving the purpose of inhibiting cell growth.

### **3.6 Effect of $\beta$ -PGG on apoptosis of hepatocellular carcinoma HepG2 cells**

A previous study revealed that apoptosis is often associated with blockage of the tumor cell cycle<sup>24</sup>. In the present study, the percentage of apoptotic cells increased gradually after treating for 48 h with different concentrations of  $\beta$ -PGG (Fig. 6). Results showed that the apoptosis rates were 36.44% and 51.02% for 100  $\mu\text{g}/\text{mL}$  and 200  $\mu\text{g}/\text{mL}$ , respectively, which were significantly higher compared to the control group. These results suggest that  $\beta$ -PGG caused apoptosis in HepG2 cells.

### **3.7 Effect of $\beta$ -PGG on the membrane potential of mitochondria in hepatocellular carcinoma HepG2 cells**

Mitochondria are common organelles in eukaryotes that not only power life, but also play a central role in apoptosis. Recent studies have shown that apoptosis is often accompanied by a decrease in MMP (mitochondrial membrane potential)<sup>25</sup>. Flow cytometry can show the change in red fluorescence in mitochondria, which indicates that the mitochondrial membrane is continuously disrupted. Herein, the mitochondrial membrane potential of hepatoma cells treated with different concentrations of  $\beta$ -PGG for 48 h changed with increasing drug concentrations, where it decreased by 25.61% at a concentration of 200  $\mu\text{g}/\text{mL}$  compared to the untreated cells. The results indicated that  $\beta$ -PGG damaged the mitochondria and caused a decrease in the mitochondrial membrane potential of the cells (Fig. 7).

### 3.8 Effect of $\beta$ -PGG on intracellular calcium ion concentration in hepatocellular carcinoma HepG2 cells

Excessive  $\text{Ca}^{2+}$  release can lead to disruption or even rupture of the outer mitochondrial membrane, thereby promoting release of apoptotic factors into the cytoplasm and inducing apoptosis<sup>26</sup>. Figure 8 shows that when the cells were treated with different concentrations of  $\beta$ -PGG for 48 h, the intracellular calcium ion concentration increased continuously as the drug concentration increased. When the drug concentration reached 200  $\mu\text{g}/\text{mL}$ , the intracellular calcium ion concentration increased significantly compared to the control group. These results suggest that  $\beta$ -PGG treatment leads to an imbalance of intracellular calcium ions in HepG2 cells and induces apoptosis.

### 3.9 Effect of $\beta$ -PGG on gene expression in hepatocellular carcinoma HepG2 cells

Figure 9 shows the expression of p53 signaling pathway-related genes in HepG2 cells after treatment with 100  $\mu\text{g}/\text{mL}$  of  $\beta$ -PGG for 48 h. The expression of *P53*, *PUMA*, *P21*, *IGF-BP3*, *CASP3*, *CASP9*, *Cytochrome C*, and *CyclinD* increased significantly in the experimental group cells compared to the control group ( $p < 0.05$ ). However, there was a decrease in the *BCL-2/BAX* ratio. These results demonstrated that the drug could induce apoptosis in hepatocellular carcinoma HepG2 cells at the genetic level by activating the p53 signaling pathway, which was consistent with the results predicted by network pharmacology.

### 3.10 Effect of $\beta$ -PGG on protein expression in hepatocellular carcinoma HepG2 cells

The expression of CASP9 and Cytochrome C proteins was upregulated in the experimental group cells compared to the control group ( $p < 0.05$ ), whereas the expression of BCL-2 was downregulated compared to the control group ( $p < 0.05$ ). The expression of P53, P21 and Cleaved CASP3 proteins was upregulated in the experimental group cells compared to the control group ( $p < 0.01$ ) and the expression of BAX was upregulated in the experimental group cells compared to the control group ( $p < 0.001$ ) (Fig. 10). This suggests that the expression of P53 protein was upregulated during the induction of apoptosis in HepG2 cells by  $\beta$ -PGG at 100  $\mu\text{g}/\text{mL}$ . In addition, upregulation of P53 protein during the induction of apoptosis by  $\beta$ -PGG was shown to promote downstream expression of PUMA protein, which in turn altered mitochondrial membrane potential, activated pro-apoptotic BCL-2 family proteins, and released Cytochrome C to induce apoptosis. The results suggest that  $\beta$ -PGG induces apoptosis in hepatocellular carcinoma HepG2 cells at the protein level by activating the p53 signaling pathway.

## 4. Discussion

1,2,3,4,6-Penta-O-galloyl- $\beta$ -D-glucose, an active substance derived from natural foods, can block the cell cycle, induce apoptosis, and exert anti-tumor effects. Studies have shown that  $\beta$ -PGG has a powerful cancer cell-killing effect and its effect is superior to that of gallic acid<sup>27</sup>. Another study found that PGG blocked the cell cycle of human multiple myeloma cells RPMI8226 in the G1 phase and induced apoptosis *in vitro*<sup>28</sup>. PGG can also downregulate the expression of *Cyclin D1*. A previous study revealed that low concentrations of PGG blocked the cycle of ER + breast cancer T-47D and BT-474 cells in S phase, whereas high concentrations of PGG blocked the cycle of cells in G1 phase<sup>14</sup>. Moreover, PGG was found to downregulate the expression of HURP and BCL-2, and increase the expression of BAX to induce apoptosis as an anti-ER breast cancer<sup>14</sup>. In colorectal cancer cells, PGG induced endogenous apoptosis by upregulating the expression of P53, P21, and cleaved CASP3<sup>28</sup>. In addition, *in vivo* experiments found that PGG cured cancer cachexia by inhibiting IR and IGF1R in pancreatic cancer cells, thereby reducing glycolytic enzymes, hepatic gluconeogenesis, skeletal muscle protein hydrolysis, and fat lipolysis in tumor grafts. Dong *et al.*<sup>29</sup> reported that PGG exerted its anti-cancerous effects *in vivo* by activating MAPK8/9/10, ERN1, and EIF2S1 signaling pathways through autophagy mediated senescence to exert its anti-hepatocellular carcinoma activity<sup>29</sup>. However, although previous studies have shown that PGG can inhibit cancer activity, the effect of PGG on liver cancer and its potential mechanism have not yet been evaluated. This study aimed at clarifying the effect of PGG on the proliferation and apoptosis of liver cancer cells, elucidating the mechanism of action of network pharmacology, and exploring the relationship between its mechanism and the p53 signaling pathway.

Network pharmacology has the potential to expand the druggable space of proteins involved in complex diseases by mapping unexplored targets of natural products, thereby identifying new therapeutic approaches for diseases<sup>30</sup>. In this study, 363 targets of PGG against liver cancer were identified using PharmMapper, SwissTargetPrediction, and GeneCards databases. GO and KEGG enrichment analyses revealed that PGG treatment of liver cancer was mainly associated with the p53 signaling pathway. It is worth noting that *P53* was identified as a tumor suppressor gene in 50% of human cancers in the late 1980s and 1990s. Specifically, genes with *P53* mutations were found in 50% of all human cancers<sup>31,32</sup>. One study revealed that *P53* is activated by various stresses to halt cancer progression by causing transient or permanent growth arrest, DNA repair, or advancing the cell death program<sup>33</sup>.

To further validate the results of network pharmacology and explore whether PGG promotes apoptosis in hepatocellular carcinoma pairs through activation of the p53 signaling pathway, an *in vitro* hepatocellular carcinoma model was established using HepG2 cells. Results obtained after performing the CCK-8 assay showed that PGG could inhibit proliferation of hepatocellular carcinoma HepG2 cells in a time-dependent manner. Flow cytometry analysis showed that PGG blocked cell growth in the S phase and increased drug concentrations blocked cells in the G0/G1 phase. P21, the first identified CDK inhibitor, binds to cell cycle protein complexes, such as A/CDK2, E/CDK2, D1/CDK4, and D2/CDK4, thereby inhibiting phosphorylation of pRB proteins<sup>34</sup>. It has been reported that P53 induces P21 to inhibit the cell cycle protein E/CDK2 in response to DNA damage, thereby inhibiting the G1/S transition<sup>35</sup>. Western blot analysis showed that PGG can lead to accumulation and activation of P21.

Apoptosis occurs when internal or external factors activate the programmed cell death process. Notably, dysregulated apoptosis is a common feature of malignant tumors. In this study, flow cytometry results showed that PGG could cause apoptosis, and the apoptotic state gradually shifted towards early apoptosis as the PGG concentration increased. After combining this result with changes in mitochondrial membrane potential and  $\text{Ca}^{2+}$  concentration, we hypothesized that apoptosis was mainly endogenous. To further investigate the relationship between  $\beta$ -PGG inhibition of apoptosis and the p53 signaling pathway, the changes of related genes and proteins on the p53 signaling pathway were first analyzed by qRT-PCR. Results showed that the mRNA expressions of *P21*, *PUMA*, *IGF-BP3*, *CASP3*, and *Cytochrome C* genes in the cells were increased with highly significant differences ( $p < 0.01$ ). In addition, the mRNA expression of *CASP9* and *PERP* was significantly increased ( $p < 0.05$ ), whereas the mRNA expression of *BAX* and *P53* showed no significant difference. Notably, the expression of *BCL-2* gene was significantly decreased ( $p < 0.05$ ). Second, western blot analysis was performed to detect the increased expression of P53, P21, Cleaved CASP3, CASP9, Cytochrome C and BAX proteins, and the decreased expression of BCL-2 protein ( $p < 0.05$ ). Activated P53 regulated the expression of downstream P21 protein, thereby resulting in an increase in P21 protein levels in HepG2 cells with a significant difference ( $p < 0.01$ ). Currently, it is increasingly becoming apparent that the p53 signaling pathway plays an important role in apoptosis<sup>26</sup>, and its activation can lead to cellular angiogenesis, inhibition of apoptosis, and DNA repair, ultimately resulting in cancer development and progression.

In summary, this study has demonstrated that  $\beta$ -PGG achieves its anti-tumor effects *in vitro* mainly through two aspects. On one hand, it affects the cell cycle by upregulating the expression of P21 gene and protein; whereas on the other hand, it induces apoptosis in HepG2 cells by increasing the expression of P53, PUMA, and CASP9 proteins, thereby causing CASP3 to shear and its shedder content to increase the ratio of BAX to BCL-2 and promote Cytochrome C release. It is worth mentioning that the mechanisms of hepatocarcinogenesis and development are complex and thus further *in vivo* experiments are needed. Overall, this study provides more possibilities for the treatment of hepatocellular carcinoma with the help of network pharmacology and provides a reference for the development of related health food products.

## Declarations

JYH drafted the manuscript, BJH drew the figures, WMR and YSJ contributed equally to plot the table, WLM, YY and WHX revised the review. All authors contributed to the article and approved the submitted version. The authors have no competing interests as defined by Springer, or other interests that might be perceived to influence the results and/or discussion reported in this paper.

## Acknowledgments

This work was supported by Primary Research & Development Plan of Hubei Province(2020BBB074) and Primary Research & Development Plan of Hubei Province(2020BBA046). The authors have no

financial interest or other potential conflict of interests. We thank home-for-researchers for editing the English of the manuscript.

## References

1. Sung H, Ferlay J, Siegel RL, Laversanne M, Soerjomataram I, Jemal A, Bray F (2021) Global Cancer Statistics 2020: GLOBOCAN Estimates of Incidence and Mortality Worldwide for 36 Cancers in 185 Countries. *CA A Cancer J Clin* caac21660. <https://doi.org/10.3322/caac.21660>
2. Lv GS, Chen L, Wang HY (2015) Research Progress and Prospect of Liver Cancer in China. *Sheng Ming Ke Xue (in Chinese)* 27:237–248
3. Yang W-S, Zeng X-F, Liu Z-N, Zhao Q-H, Tan Y-T, Gao J, Li H-L, Xiang Y-B (2020) Diet and Liver Cancer Risk: A Narrative Review of Epidemiological Evidence. *Br J Nutr* 124(3):330–340
4. Mayne ST, Playdon MC, Rock CL (2016) Diet, Nutrition, and Cancer: Past, Present and Future. *Nat reviews Clin Oncol* 13(8):504–515
5. Di Furia L, Rusciano MR, Leonardini L, Rossi P, Giammarchi C, Vittori E, Tilocca S, Russo FL, Montuori P, Triassi M (2015) A Nutritional Approach to the Prevention of Cancer: From Assessment to Personalized Intervention. *Translational Medicine@ UniSa* 13:33
6. Tueros I, Uriarte M (2018) Innovative Food Products for Cancer Patients: Future Directions. *J Sci Food Agric* 98(5):1647–1652
7. Sharma A, Kaur M, Katnoria JK, Nagpal AK (2018) Polyphenols in Food: Cancer Prevention and Apoptosis Induction. *Curr Med Chem* 25(36):4740–4757
8. Yang M, Memon KH, Lateef M, Na D, Wan S, Eric D, Zhang L, Jiang T (2016) 1, 2, 3, 4, 6-Pentakis [-O-(3, 4, 5-Trihydroxybenzoyl)]- $\alpha$ ,  $\beta$ -D-Glucopyranose (PGG) Analogs: Design, Synthesis, Anti-Tumor and Anti-Oxidant Activities. *Carbohydrate Research* 430, 72–81
9. Jin F, Ma K, Chen M, Zou M, Wu Y, Li F, Wang Y (2015) Pentagalloylglucose Blocks the Nuclear Transport and Nucleocapsid Egress Process to Inhibit Hsv-1 Infection. *Japanese Journal of Infectious Diseases* JJID. 2015.137
10. Kiss AK, Filipek A, Żyżyńska-Granica B, Naruszewicz M (2013) Effects of Penta-O-galloyl- $\beta$ -D-glucose on Human Neutrophil Function: Significant Down-regulation of L-selectin Expression. *Phytother Res* 27(7):986–992
11. Zhao Y, Wang B, Zhang S, Yang S, Wang H, Ren A, Yi E (2015) Isolation of Antifungal Compound from *Paeonia Suffruticosa* and Its Antifungal Mechanism. *Chin J Integr Med* 21(3):211–216
12. Bruno E, Pereira C, Roman KP, Takiguchi M, Kao P-Y, Nogaj LA, Moffet DA (2013) IAPP Aggregation and Cellular Toxicity Are Inhibited by 1, 2, 3, 4, 6-Penta-O-Galloyl- $\beta$ -D-Glucose. *Amyloid* 20(1):34–38
13. Hu H, Lee H-J, Jiang C, Zhang J, Wang L, Zhao Y, Xiang Q, Lee E-O, Kim S-H, Lü J (2008) Penta-1, 2, 3, 4, 6-O-Galloyl- $\beta$ -d-Glucose Induces P53 and Inhibits STAT3 in Prostate Cancer Cells in Vitro and Suppresses Prostate Xenograft Tumor Growth in Vivo. *Mol Cancer Ther* 7(9):2681–2691

14. Xiang Q, Tang J, Luo Q, Xue J, Tao Y, Jiang H, Tian J, Fan C (2019) In Vitro Study of Anti-ER Positive Breast Cancer Effect and Mechanism of 1, 2, 3, 4-6-Pentyl-O-Galloyl-Beta-D-Glucose (PGG). *Biomed Pharmacother* 111:813–820
15. Holtz JN, Silverman RK, Tay KJ, Browning JT, Huang J, Polascik TJ, Gupta RT (2018) New Prostate Cancer Prognostic Grade Group (PGG): Can Multiparametric MRI (MpMRI) Accurately Separate Patients with Low-, Intermediate-, and High-Grade Cancer? *Abdom Radiol* 43(3):702–712
16. Yang J, Wang F, Chen X, Qiu S, Cui L, Hu L (2019)  $\beta$ -Pentagalloyl-Glucose Sabotages Pancreatic Cancer Cells and Ameliorates Cachexia in Tumor-Bearing Mice. *Am J Chin Med* 47(03):675–689
17. Hopkins AL *Network Pharmacology: The next Paradigm in Drug Discovery*. *Nature chemical biology* 2008, 4 (11),682–690
18. Chin C-H, Chen S-H, Wu H-H, Ho C-W, Ko M-T, Lin C-Y (2014) CytoHubba: Identifying Hub Objects and Sub-Networks from Complex Interactome. *BMC Syst Biol* 8(4):1–7
19. Wu T, Hu E, Xu S, Chen M, Guo P, Dai Z, Feng T, Zhou L, Tang W, Zhan L (2021) ClusterProfiler 4.0: A Universal Enrichment Tool for Interpreting Omics Data. *The Innovation* 2(3):100141
20. Yu G, Enrichplot (2019) : Visualization of Functional Enrichment Result.R package version 1 (1)
21. Mailund TR (2019) *Data Science Quick Reference*. Springer
22. Lacroix M, Riscal R, Arena G, Linares LK, Le Cam L (2020) Metabolic Functions of the Tumor Suppressor P53: Implications in Normal Physiology, Metabolic Disorders, and Cancer. *Mol metabolism* 33:2–22
23. Liang Y, Yan C, Schor NF (2001) Apoptosis in the Absence of Caspase 3. *Oncogene* 20(45):6570–6578
24. Li N, Fan L-L, Sun G-P, Wan X-A, Wang Z-G, Wu Q, Wang H (2010) Paeonol Inhibits Tumor Growth in Gastric Cancer in Vitro and in Vivo. *World J Gastroenterology: WJG* 16(35):4483
25. Ly JD, Grubb DR, Lawen A (2003) The Mitochondrial Membrane Potential ( $\Delta\psi_m$ ) in Apoptosis; an Update. *Apoptosis* 8(2):115–128
26. Giorgi C, Baldassari F, Bononi A, Bonora M, De Marchi E, Marchi S, Missiroli S, Patergnani S, Rimessi A, Suski JM (2012) Mitochondrial Ca<sup>2+</sup> and Apoptosis. *Cell Calcium* 52(1):36–43
27. Yang M, Memon KH, Lateef M, Na D, Wan S, Eric D, Zhang L, Jiang T (2016) 1, 2, 3, 4, 6-Pentakis [-O-(3, 4, 5-Trihydroxybenzoyl)]- $\alpha$ ,  $\beta$ -D-Glucopyranose (PGG) Analogs: Design, Synthesis, Anti-Tumor and Anti-Oxidant Activities. *Carbohydrate Research* 430, 72–81
28. Tseeleesuren D, Kant R, Yen C-H, Hsiao H-H, Chen Y-MA (2018) 1, 2, 3, 4, 6-Penta-O-Galloyl-Beta-D-Glucopyranoside Inhibits Proliferation of Multiple Myeloma Cells Accompanied with Suppression of MYC Expression. *Front Pharmacol* 9:65
29. Dong Y, Yin S, Jiang C, Luo X, Guo X, Zhao C, Fan L, Meng Y, Lu J, Song X (2014) Involvement of Autophagy Induction in Penta-1, 2, 3, 4, 6-O-Galloyl- $\beta$ -D-Glucose-Induced Senescence-like Growth Arrest in Human Cancer Cells. *Autophagy* 10(2):296–310

30. Kibble M, Saarinen N, Tang J, Wennerberg K, Mäkelä S, Aittokallio T (2015) Network Pharmacology Applications to Map the Unexplored Target Space and Therapeutic Potential of Natural Products. *Nat Prod Rep* 32(8):1249–1266
31. Olivier M, Hollstein M, Hainaut P (2010) TP53 Mutations in Human Cancers: Origins, Consequences, and Clinical Use. *Cold Spring Harb Perspect Biol* 2(1):a001008
32. Robles AI, Harris CC (2010) Clinical Outcomes and Correlates of TP53 Mutations and Cancer. *Cold Spring Harb Perspect Biol* 2(3):a001016
33. Stegh AH (2012) Targeting the P53 Signaling Pathway in Cancer Therapy—the Promises, Challenges and Perils. *Expert Opin Ther Targets* 16(1):67–83
34. Choi W-I, Kim M-Y, Jeon B-N, Koh D-I, Yun C-O, Li Y, Lee C-E, Oh J, Kim K, Hur M-W (2014) Role of Promyelocytic Leukemia Zinc Finger (PLZF) in Cell Proliferation and Cyclin-Dependent Kinase Inhibitor 1A (P21WAF/CDKN1A) Gene Repression. *J Biol Chem* 289(27):18625–18640
35. Karimian A, Ahmadi Y, Yousefi B (2016) Multiple Functions of P21 in Cell Cycle, Apoptosis and Transcriptional Regulation after DNA Damage. *DNA Repair* 42:63–71

## Figures

### Figure 1

**Pharmacological networks of  $\beta$ -PGG and liver cancer.** (a) 2D structure of  $\beta$ -PGG. (b) Venn diagram showing the drug-disease interactions. (c) The “ $\beta$ -PGG-target-hepatocellular carcinoma” network.



**Figure 2**

**PPI network diagram and identified hub genes.** PPI map showing key genes, changes are presented based on size and color of degree value.

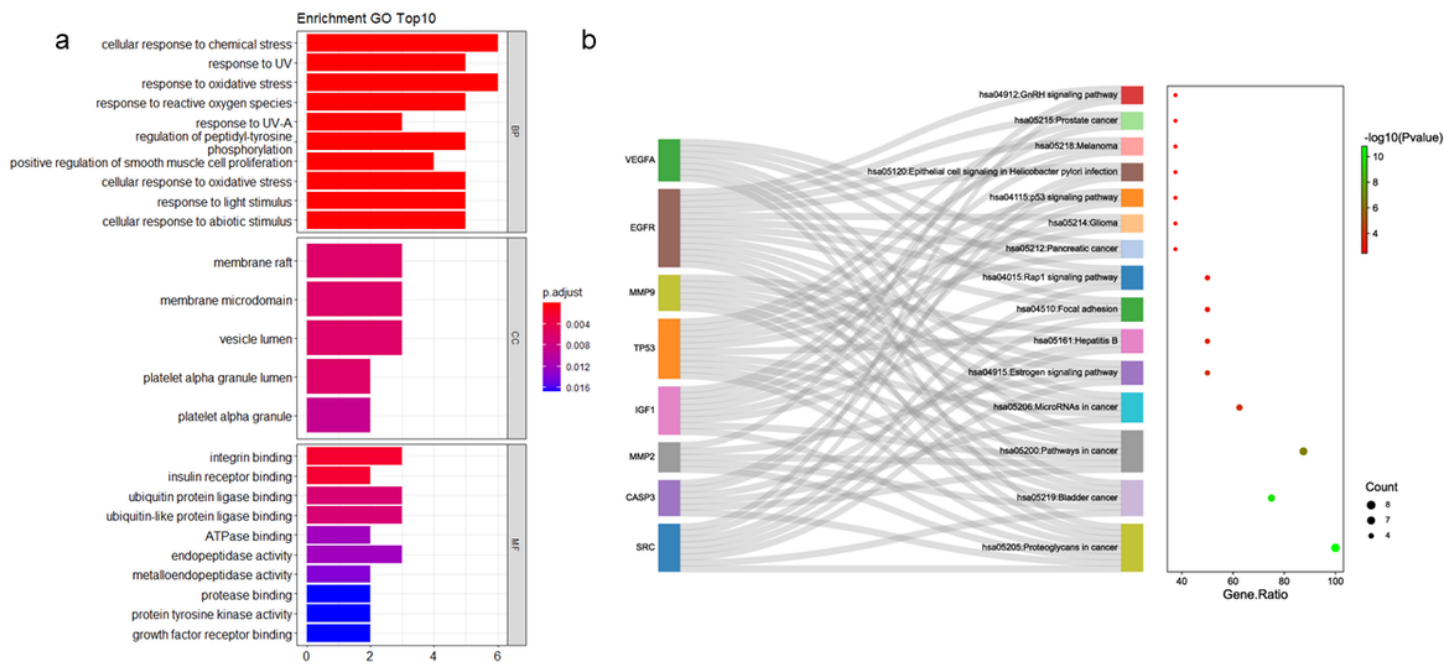
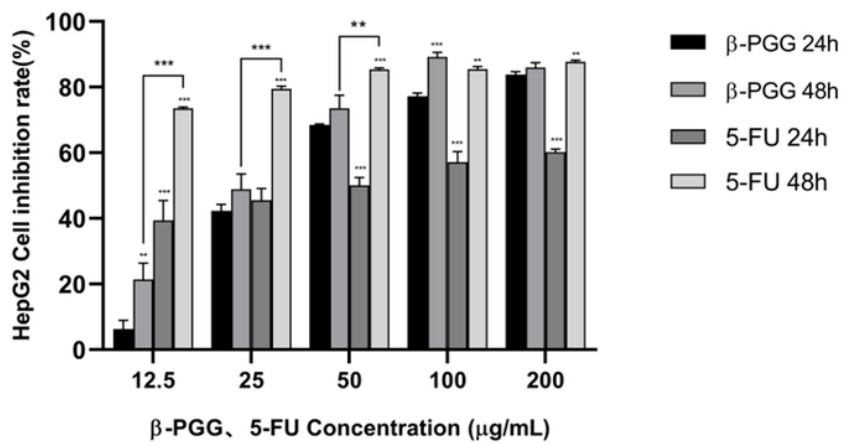


Figure 3

GO and KEGG pathway analysis of hub genes. (A) GO analysis. (B) KEGG pathway analysis.



**Figure 4**

**Effect of  $\beta$ -PGG on proliferation of HepG2 cells.** HepG2 cells were treated with different concentrations of  $\beta$ -PGG and different concentrations of 5-FU (12.5, 25, 50, 100 and 200  $\mu\text{g}/\text{mL}$ ) for 24 h and 48 h, and detected by CCK-8 assay. (\*\* $p < 0.01$ , \*\*\* $p < 0.001$  vs.  $\beta$ -PGG 24 h).

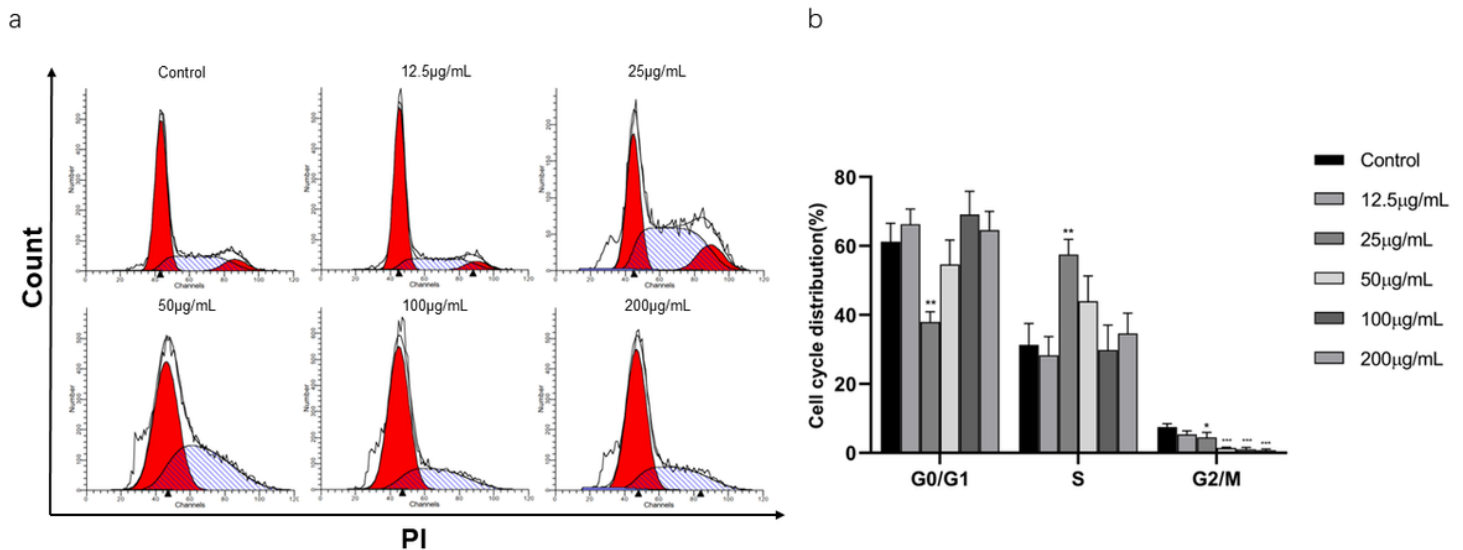


**Figure 5**

**Effects of 1,2,3,4,6-Penta-O-galloyl- $\beta$ -D-glucose on HepG2 cell cycle.** (a) Intracellular fluorescence intensity of HepG2 cells cultured with 1,2,3,4,6-Penta-O-galloyl- $\beta$ -D-glucose (0, 12.5, 25, 50, 100 and 200  $\mu\text{g}/\text{mL}$ ) for 48 h. (b) Average fluorescence intensity of HepG2 cells. (\* $p < 0.05$ , \*\* $p < 0.01$ , \*\*\* $p < 0.001$  vs. 0  $\mu\text{g}/\text{mL}$ )

**Figure 6**

**Effects of 1,2,3,4,6-Penta-O-galloyl- $\beta$ -D-glucose on apoptosis of HepG2 cells.** (a) FITC-Annexin V/PI double-staining flow cytometry showing apoptosis rate of HepG2 cells after treatment with 1,2,3,4,6-Penta-O-galloyl- $\beta$ -D-glucose and 5-FU (0, 12.5, 25, 50, 100 and 200  $\mu\text{g}/\text{mL}$ ) for 48 h. (b) Average apoptosis rate of HepG2 cells. (\*\* $p < 0.01$ , \*\*\* $p < 0.001$  vs. 0  $\mu\text{g}/\text{mL}$ )

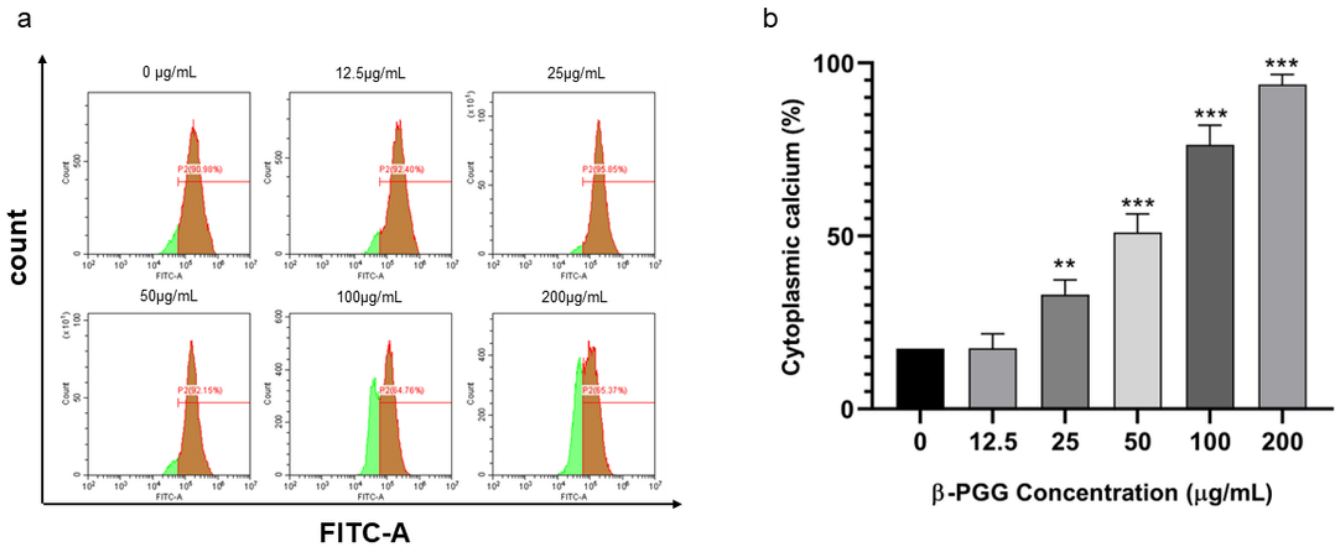


**Figure 7**

**Effects of 1,2,3,4,6-Penta-O-galloyl-β-D-glucose on mitochondrial membrane potential in HepG2 cells.** HepG2 cells were incubated with different concentrations of 1,2,3,4,6-Pentagram-β-D-glucose for 48 h.  $\Delta\psi_m$  was evaluated using JC-10 in treated cells. (a)  $\Delta\psi_m$  after treatment of cells with 0, 12.5, 50, 100, 200 μg/mL β-PGG (b) Average mitochondrial membrane potential rate of HepG2 cells. (\*\* $p < 0.01$ , \*\*\* $p < 0.001$  vs. 0 μg/mL)

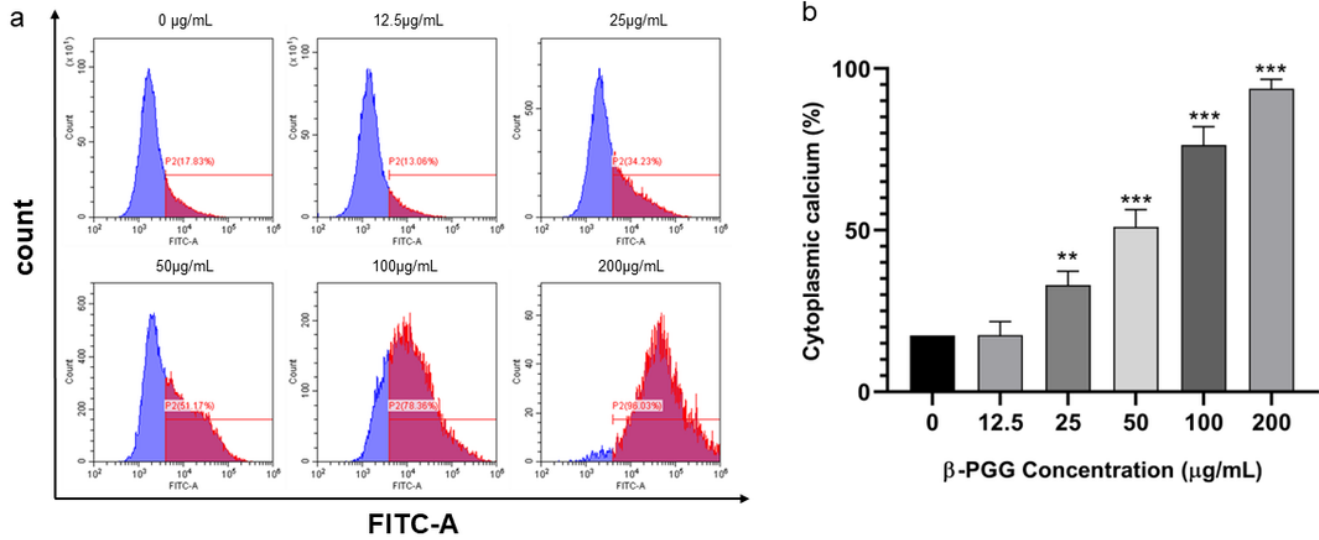


**Figure 8**

**Effect of 1,2,3,4,6-Penta-O-galloyl-β-D-glucose on intracellular Ca<sup>2+</sup> concentration in HepG2 cells.** HepG2 cells were incubated with different concentrations of 1,2,3,4,6-Penta-O-galloyl-β-D-glucose for 48 h. Fluo 3-AM assay was performed to determine Ca<sup>2+</sup> concentration. (a) Intracellular Ca<sup>2+</sup> concentration after treatment of cells with 0, 12.5, 50, 100, 200 μg/mL (b) Average Cytoplasmic calcium rate of HepG2 cells. (\**p*<0.05, \*\**p*<0.01, \*\*\**p*<0.001 vs. 0 μg/mL)

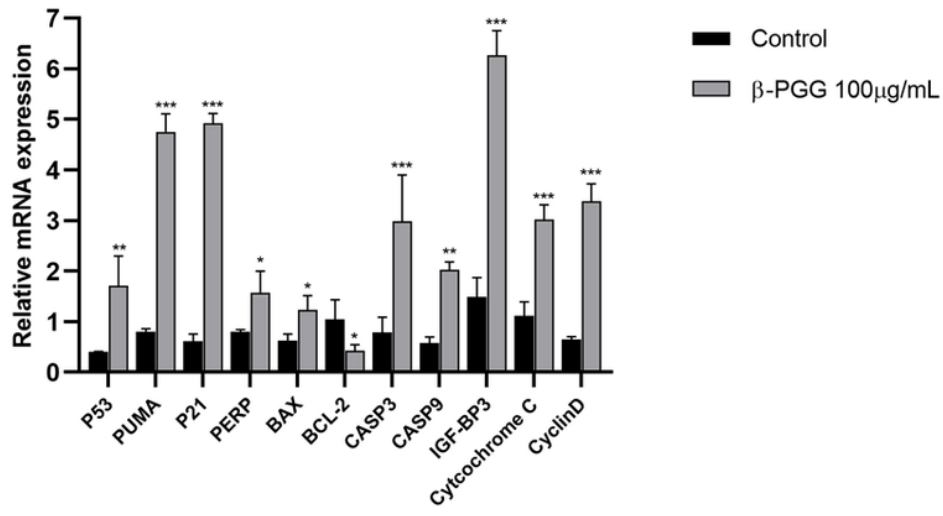


**Figure 9**

**Expression levels of apoptotic-related genes in HepG2 cells.** qRT-PCR was used to determine mRNA levels of apoptosis-related genes in HepG2 cells. Expression levels of *P21*, *PERP*, *IGF-BP3*, *PUMA*, *BAX*, *BCL-2*, *CASP9*, *Cyclin D*, *Cytochrome C*, *CASP3*, *P53*. Cells were treated with 100 μg/mL 1,2,3,4,6-Penta-O-galloyl-β-D-glucose for 24 h. (\* $p < 0.05$ , \*\* $p < 0.01$ , \*\*\* $p < 0.001$  vs. control)

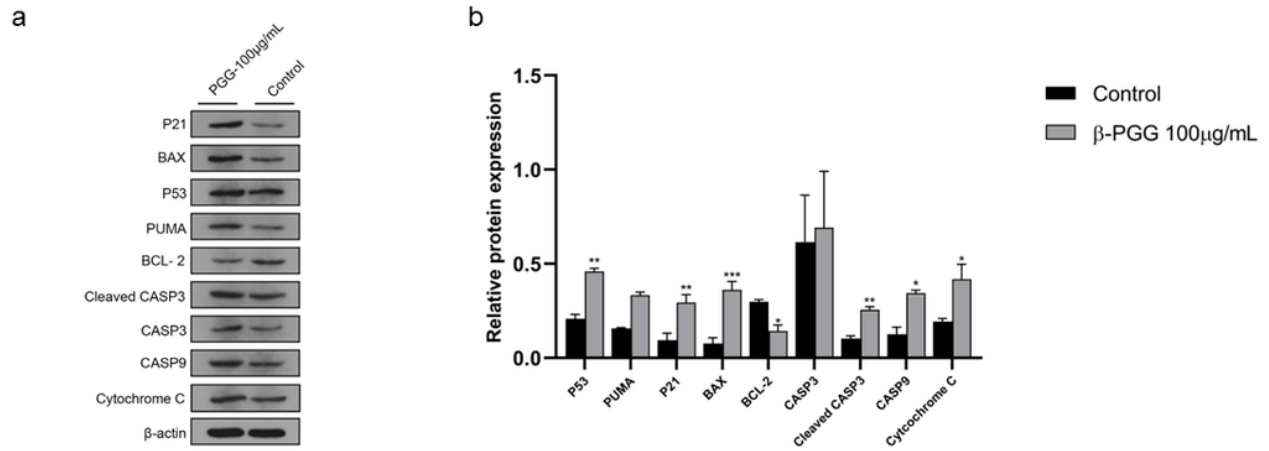


**Figure 10**

**Expression levels of apoptotic-related proteins in HepG2 cells.** (a) Expression levels of BAX, BCL-2, CASP3, Cleaved CASP3, CASP9, Cytochrome C, P21, P53, PUMA in HepG2 cells as determined by western blot. Cells were treated with 100 μg/mL 1,2,3,4,6-Penta-O-galloyl-β-D-glucose for 24 h. (b) The average of P21, BAX, P53, PUMA, BCL-2, PUMA, CASP3, Cleaved CASP3, CASP9 and Cytochrome C proteins band grayscale. Cells were treated with 100 μg/mL 1,2,3,4,6-Penta-O-galloyl-β-D-glucose for 24 h. (\* $p < 0.05$ , \*\* $p < 0.01$ , \*\*\* $p < 0.001$  vs. control)

## Supplementary Files

This is a list of supplementary files associated with this preprint. Click to download.

- [Westernblot.xlsx](#)